International Journal of Computing and Digital Systems
ISSN (2210-142X)
Int. J. Com. Dig. Sys. 11, No.1 (Jan-2022)

https://dx.doi.org/10.12785/ijcds/110115

Comparison of Fractal Dimension and Wavelet Transform Methods in Classification of Stress State from EEG Signals

Fatimah Abdul Hamid[1,2], Mohamad Naufal Mohamad Saad[2] and Norshakila Haris[1]

[1]*Marine and Electrical Engineering Technology Section, Malaysian Institute of Marine Engineering Technology, Universiti Kuala Lumpur, Perak, Malaysia*

[2]*Centre for Intelligent Signal and Imaging Research (CISIR), Electrical and Electronics Engineering Department, Universiti Teknologi PETRONAS, Perak, Malaysia*

Received 28 Mar. 2021, Revised 28 Jun 2021, Accepted 20 Sep. 2021, Published 9 Jan. 2022

Abstract: Stress is a significant issue in everyday life that affects both physical and mental health. There are different approaches to stress classification. This research examines the implementation of the fractal dimension (FD) method as one of the features for stress state classification using brain signals. Consequently, the comparison between FD and wavelet transform has been conducted using electroencephalogram (EEG) signals recorded during the Stroop Colour Word Test (SCWT). The comparison results show that the FD is better in the classification of the stress state. The highest F1 score has been obtained using FD with quadratic support vector machine (SVM) in average 83.03% for the comparison between baseline session and different stress states. Besides, FD with medium Gaussian SVM has the highest F1 score, on average 83.36%, for comparison between various stress states.

Keywords: Stress, Fractal Dimension, Wavelet Decomposition

1. Introduction

Most people experience stress in their daily life. Although there is a strong relationship between stress and mental health, psychological stress and related emotions, such as frustration, anxiety, and depression, may also have adverse effects on physical health. An electroencephalogram (EEG) is an electrophysiological monitoring system for recording electrical activity in the cortex. The EEG was initially designed to test human brain cortical function. Since Hans discovered the alpha rhythm, the essence of the background activity in human brains and how it reflects action and cognitive processes have been of primary interest to scientists [1], [2].

Numerous studies have shown the association between the EEG pattern and stress level [3], [4], [5], [6], [7]. In [8], a combination of time-domain and frequency-domain analysis using wrapper-based algorithms as features and Boruta as feature selector was proposed to identify stress levels using EEG signals. These features are then classified using k-nearest neighbor (KNN) with an accuracy of 73.38%. Other studies show that 82% accuracy achievement using higher-order spectra (HOS) as stress recognition with genetic algorithm for optimal selection of features and classification of support vector machine (SVM) [9]. For two stages of stress recognition, the authors in [10] chose to combine fractal dimensions and statistical features. The accuracy recorded was 85.71% using SVM as a classifier. Meanwhile, [11] proposed root means square voltage computed as a feature in the beta, alpha, and theta band. These features were then used as inputs for logistic regression and the KNN classifier, yielding a mean accuracy of 73.47%. The authors of [12] found that discrete cosine transform (DCT) was used along with KNN. The average classification rate indicated was 72% for cognitive stress recognition. The author suggested a fixed windowing approach of time-domain and frequency-domain features in [13], with the SVM classifier achieving an accuracy of 80.32%. Recently, [14] suggested that alpha asymmetry as a feature using SVM as classifier with accuracy up to 85.20%. All previous findings mentioned above are listed in Table I.

This paper compares two feature extractions (fractal dimension and wavelet transform) and evaluates the stress classification states from the EEG signals.

2. Materials And Methods

Figure 1 indicates the overall process classification of stress state using EEG signals that have been developed in this research. Details of the process are explained in the

E-mail address: fatimahah@unikl.edu.my

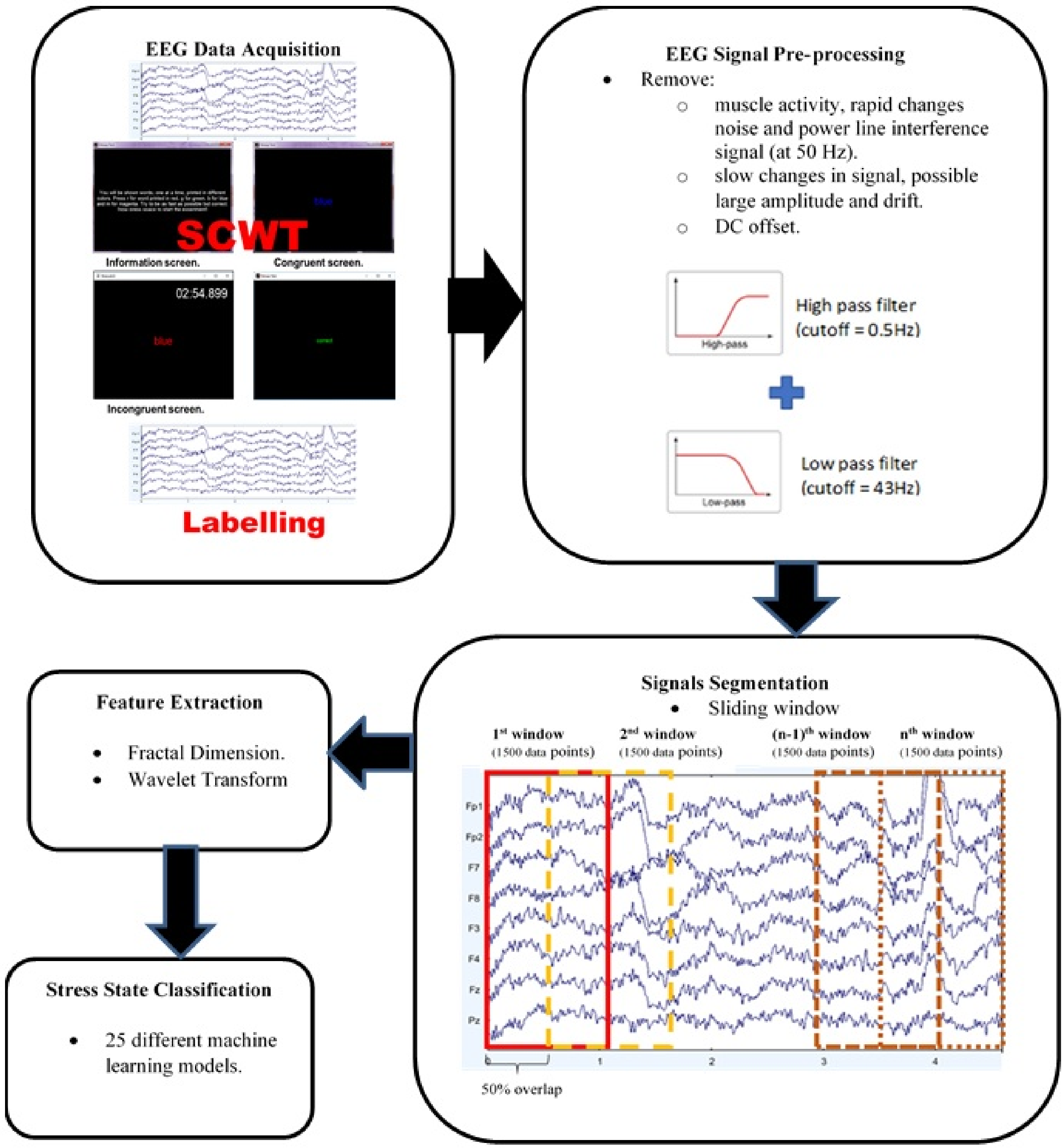

Figure 1. Overall illustration of stress state classification process

TABLE I. Summary of previous researches on stress state classification

Ref.	Features	Classifier	Accuracy
[8] 2019	Time-domain (statistical parametric) & frequency-domain (wavelet-based) using wrapper-based	KNN	73.38
[9] 2010	Higher-order spectra (HOS)	SVM	82.00
[10] 2016	Fractal dimension & statistical	SVM	85.71
[11] 2013	Root means square voltage of beta, alpha, and theta band	Logistic regression & KNN	73.46
[12] 2015	Discrete cosine transforms	KNN	72.00
[13] 2018	Time-domain & frequency-domain	Gaussian SVM	80.32
[14] 2020	Alpha asymmetry	SVM, Naïve Bayes, KNN, logistic regression, & multilayer perception (MLP)	85.20

following sub-topics.

A. *Participants*

The study included twelve healthy volunteers between the ages of 20 and 21. All the participants are free of any personal history of neurological or mental illness, pre-existing medical condition, chronic medical use, or any other non-medical substances that could impair cognitive function before the screening. Participants with a previous history of working with the Stroop Colour Word Test (SCWT) will be acknowledged. The nature and design of the study were clarified to all participants.

B. *EEG Data Acquisition*

The EEG signals were acquired using ENOBIO 8 channels with resolution 24 bits – 0.05 μV. All these dry electrodes are placed on the scalp (Figure 2) using a neoprene cap based on the International 10-20 system channel location [15], [16], [17]. The ground electrode is placed at the mastoid using sticktrode. The sampling rate was fixed at 500 samples per second for all channels.

C. *Tasks*

The task for this study was created using MATLAB based on [18], [19], [20]. Figure 3 depicts the flow of the SCWT test, which is designed to generate four different levels of stress: baseline state (BS), low stress (L1), mild stress (L2), and higher stress (L3) state. SCWT was used as a stressor as a commonly used method to induce stress [21]. The followings are the details of the stress-based evaluation session:

- *Introductory Session (IS)*: This condition allows the participants to become familiarized with the test background. The task method was explained, and guidelines for administering the SCWT task were provided.
- *Baseline Session (BS)*: This is referred to as the baseline session. Participants were instructed to relax and remain their eyes open for three minutes during this section. The aim was for the participants to be in the most relaxed state possible. Throughout this time, they relaxed and listened to Bach's Harpsichord Concerto No. 5 in F Minor BWV 1056.
- *Session 1 (L1)*: In this segment, a low level of stress is induced. Participants were given a simple and non-time-limited task. Twenty printed words describing four types of colors: red, green, blue, and magenta, are displayed to the participant. The printed words in the congruent (CS) and incongruent (ICS) sections have identical and dissimilar ink colors. Instead of acknowledging written words, participants were asked to recognize the ink colors.
- *Session 2 (L2)*: With a three-minute response time, this segment was designed to induce mild stress. The standard step was the same as L1, except that participants had to respond within the time limit (3 minutes). It was predicted that the participants would be more stressed than L1.
- *Session 3 (L3)*: This part resulted in a higher stress state than L2. The standard step was similar to L1 and L2 but with a shorter time limit (1.5 minutes).

D. *EEG Signals Pre-Processing*

EEG signals recorded at different locations on the scalp are generally contaminated with noise and artifacts (e.g., ocular (EOG), muscular (EMG), drifting in electrode impedance, vascular (ECG), gloss kinetic artifacts, sweating, line noise, and channel noise). The complete elimination of artifacts would also extract some valuable details from EEG signals. Therefore, artifact removal should be canceling or fixing artifacts without altering the signal interest. This pre-processing part is achieved mainly in two different methods: filtering and regression or separating/decomposing EEG data into other domains [22].

In this work, the filtering method is used for removing

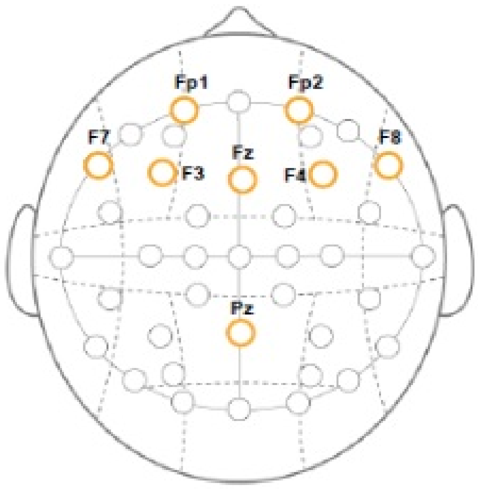

Figure 2. ENOBIO 8 channel location for Fp1, Fp2, F7, F8, F3, F4, Fz, and Pz.

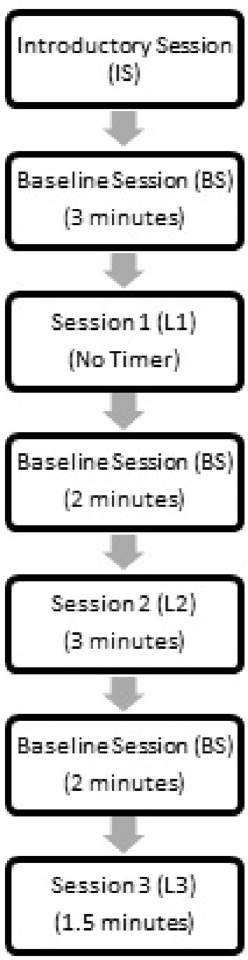

Figure 3. The process of the SCWT experiment

the noise and artifacts. A bandpass filter with a cutoff frequency between 0.5 Hz and 43 Hz is used to eliminate most present extrinsic artifacts such as slow changes in the signal, possible large-amplitude, drift, muscle activity, rapid changes in noise, and power line interference signal at 50 Hz.

E. Signals Segmentation

Segmentation data into various windows establishes a single continuous section covering all-action sequence data (i.e., sliding window approach) and improved classification accuracy [13], [23]. Then, features were extracted from these windowed sections and used in a machine-learning algorithm to categorize a testing section.

The EEG signals in this work are segmented into 50 percent overlapping 3-second windows size based on previous researcher findings [23]. The sliding window size was 1500 data points as the EEG signals sampling rate was 500 Hz.

F. Feature Extraction

The next process is to identify useful features that can be applied to detect stress. The methods used in this study are the fractal dimension, and wavelet transforms.

1) *Fractal Dimension*: In this works, the fractal dimension based on Higuchi's algorithm is used as it showed promising results [24]. Higuchi's algorithm [25] is based on calculating the mean length of the curve /(k) by using a segment of k samples as a unit of measure. From the time series X(1), X(2), ..., X(N), the algorithm constructs a new time series. Each of them, X_m^k is described as a new time series in Equation 1:

$$X_m^k : X(m), X(m+k), X(m+2*k), ..., \quad (1)$$
$$X\left(m + int\left(\frac{(N-m)}{k}\right)*k\right), m = 1, 2, 3, ..., k$$

where m and k are the integers of initial time and interval time, respectively. For example, if k=5 and N=500, five-time series are produced as Equation 2:

$$X_1^5 : X(1), X(6), X(11), ..., X(491), X(496) \quad (2)$$
$$X_2^5 : X(2), X(7), X(12), ..., X(492), X(497)$$
$$X_3^5 : X(3), X(8), X(13), ..., X(493), X(498)$$
$$X_4^5 : X(4), X(9), X(14), ..., X(494), X(499)$$
$$X_5^5 : X(5), X(10), X(15), ..., X(495), X(500)$$

Then the length, $L_m(k)$, of each curve X_m^k is defined as Equation 3:

$$L_m(k) = \tag{3}$$
$$\left[\frac{\left(\sum_{i=1}^{int((N-m)/k)} \left| X(m+i*k) - X(i-1)*k \right| (n-1) \right)}{int\left(\frac{(N-m)}{k}\right)*k} \right]$$

where N is the total number of data sequence X and $int((N-m)/k)*k$ is a normalization factor. The k mean length is determined as the average length of k length $L_m(k)$ for m=1,2,3,...,k. This process is repeated for each k ranging from 1 to k_{max} with an average duration of each k. In the curve of ln(L(k)) versus ln(1/k), the gradient of the least-square linear best fit is the best approximation of the fractal dimension.

2) *Wavelet Transformation*: Wavelet transform (WT) extract a signal into a set of details along with approximations of signals that cannot be accomplished either by Fast Fourier Transform (FFT) or by Short Time Fourier Transform (STFT). These are obtained by dilation and contraction and shifts from a single prototype wavelet called a mother wavelet.
The function of the mother wavelet $\psi_{a,b}(t)$ at time a and scale b is defined as Equation 4:

$$\psi_{a,b}(t) = \frac{1}{\sqrt{a}}\psi\left(\frac{t-b}{a}\right) \tag{4}$$

where $a, b \epsilon R, a > b$, and R is the wavelet space. $1/\sqrt{a}$ is used to normalize the energy so that it remains constant for various a and b values. As a result, 'a' represents the scaling factor that captures the local frequency information, and 'b' represents the translation factor that localizes the wavelet basis function at time t=b and its surroundings.
If x(t) is a time-based input signal, then continuous WT (CWT) can write as Equation 5:

$$CWT(a,b) = \int x(t)\psi^*_{a,b}(t)dt \tag{5}$$

where * represent the complex conjugate.
Time-frequency representation is conducted to split the frequency domain in the middle by repetitively filtering the signal with a pair of wavelet filters. Precisely, a WT decomposes the signals into approximation coefficients (CA) and detailed coefficients (CD). The CA is then split up into a new CA and CD. This process is accomplished to generate a set of CA and CD iteratively.
Considering the Daubechies order 4 (dB4) function is used for decomposing the EEG signals in this work, resulting in the discrete wavelet transform decomposition, as shown in Table II. This function has been chosen because it has time-frequency localization properties near to optimal [26], [27]. Usually, the EEG signals are divided into five frequency bands (δ, θ, α, and γ) [26] (Table II).

TABLE II. EEG signals decomposition of different levels frequency band for Daubechies order 4 with a sampling frequency of 500 Hz

Decomposed Levels	Frequency Range (Hz)	Frequency Band
D1	89.2875 – 178.5750	Noise
D2	44.6430 – 89.2875	Noise
D3	22.3219 – 44.6438	Gamma(Noise)
D4	11.1609 – 22.3219	Beta
D5	5.5805 – 11.1609	Alpha
D6	2.7902 - 5.5805	Theta
A5	0 – 2.7902	Delta

G. Stress State Classification

EEG signals classification shall consist of the following steps:

- Pre-processing of signals: This involves determining fractal dimension and wavelet coefficients in the present work, using the sub-band coding scheme mentioned above. These outputs will be used to define the signal as 'features'.
- Thus, features extracted from the pre-processing operation are entered into 25 different machine learning (ML) (Table III, which performs classification over a set of extracted parameters, in this case, a set of fractal dimensions or wavelet coefficients.

The classification was done using two stress levels dependent on the SCWT session (normal-mild, mild-stressful, normal-stressful). The feature vector for the training machine learning model is specified as Equation 6 and Equation 7 for FD features, while Equation 8 and Equation 9 refer to the CD of wavelet transform feature extraction vector features. 10-fold cross-validation includes breaking the data to 10-fold, then training to 9-folds, and checking to the remaining 1-fold as validation. The average accuracy and F1 scores of these 10 iterations were calculated for each feature. Here, we only consider CD for an alpha band (D5) as increasing the alpha band's power would represent calming and aware conditions. Meanwhile, decreasing the alpha band's power and increasing the power of the beta band would mean that people are doing intense tasks such as doing mental arithmetic, answering examinations, and so on [28], [29], [30].

$$RSS1_{1-7} = \begin{bmatrix} FD_{RS(1)} & FD_{RS(2)} & \dots & FD_{RS(7)} \\ \vdots & \vdots & \vdots & \vdots \\ FD^{CS}_{S1(1)} & FD^{CS}_{S1(2)} & \dots & FD^{CS}_{S1(7)} \\ \vdots & \vdots & \vdots & \vdots \end{bmatrix} \tag{6}$$

TABLE III. Machine learning used for stress classification and description

No.	Machine Learning	Description
1	Fine tree (FT)	Supervised-Regression
2	Medium tree (MT)	Supervised-Regression
3	Coarse tree (CT)	Supervised-Regression
4	Linear discriminant (LD)	Supervised–Classification
5	Quadratic discriminant (QD)	Supervised–Classification
6	Logistic regression (LR)	Supervised-Regression
7	Naïve Bayes Gaussian (NBG)	Supervised–Classification
8	Naïve Bayes Kernel (NBK)	Supervised–Classification
9	Linear support vector machine (LSVM)	Supervised–Classification
10	Quadratic SVM (QSVM)	Supervised–Classification
11	Cubic SVM (CSVM)	Supervised–Classification
12	Fine Gaussian SVM (FGSVM)	Supervised–Clustering
13	Medium Gaussian SVM (MGSVM)	Supervised–Clustering
14	Coarse Gaussian SVM (CGSVM)	Supervised–Clustering
15	Fine K-Nearest Neighbor (FKNN)	Supervised–Classification
16	Medium KNN (MKNN)	Supervised–Classification
17	Coarse KNN (CKNN)	Supervised–Classification
18	Cosine KNN (CsKNN)	Supervised–Classification
19	Cubic KNN (CbKNN)	Supervised–Classification
20	Weighted KNN (WKNN)	Supervised–Classification
21	Boosted trees (BT)	Supervised-Regression
22	Bagged trees (BgT)	Supervised-Regression
23	Subspace discriminant (SD)	Supervised–Classification
24	Subspace KNN (SKNN)	Supervised–Classification
25	RUSBoosted trees (RUSBT)	Supervised-Regression

$$XY_{1-7} = \begin{bmatrix} FD^a_{X(1)} & FD^a_{X(2)} & \cdots & FD^a_{X(7)} \\ \vdots & \vdots & \vdots & \vdots \\ FD^b_{Y(1)} & FD^b_{Y(2)} & \cdots & FD^b_{Y(7)} \\ \vdots & \vdots & \vdots & \vdots \end{bmatrix} \tag{7}$$

a or b representing CS or ICS symbolizes a congruent segment and an incongruent segment, X or Y symbolizes SCWT session: RS, S1, S2, and S3, and 1 to 7 represents EEG channels Fp1, Fp2, F7, F8, F3, F4, and Fz. Each vector represents the features of each window in the series.

$$RSS1 = \begin{bmatrix} CD_{RS} & CD_{RS} \\ \vdots & \vdots \\ CD^{CS}_{S1} & CD^{CS}_{S1} \\ \vdots & \vdots \end{bmatrix} \tag{8}$$

$$XY = \begin{bmatrix} CD^a_X & CD^a_X \\ \vdots & \vdots \\ CD^b_Y & CD^b_Y \\ \vdots & \vdots \end{bmatrix} \tag{9}$$

where a or b represents CS or ICS for congruent section and incongruent section, X or Y symbolizes the RS, S1, S2, and S3 session in the SCWT session. Each vector represents the features of each window in a series.

3. Results And Discussion

In this research, the length of the SCWT session varies from one subject to another. It is a subject-dependent task. Figure 4 and Figure 5 present the cross-validation results obtained after performing training and testing using machine learning methods previously stated for stress states classification with FD and WT features between baseline sessions (BS) and different stress state (L1, L2, and L3). The results show that the highest F1 score and accuracy were obtained using FD features with quadratic SVM classifier (F1 scores:80.21% for BS-L1 session, 83.44% for BS-L2 session; Accuracy: 79.77% for BS-L1, 84.28% for BS-L2) and quadratic discriminant (F1 scores: 86.89%, accuracy: 86.27% for BS-L3 session). From these results, it is clear that the stress level increases with an increase in FD accuracy and F1 scores while WT shows an increasing trend between L1 to L2 but decreases when going to decrease in WT accuracy. Different stress states significantly influence average accuracy and F1 scores due to decreased alpha power and increases in theta power. This result is in agreement with a similar finding reported by [30].

The comparison between different stress levels (L1, L2, and L3) can be seen in Figure 6 and Figure 7. In general, the classification trend between stress levels is similar compared to the trends observed previously in the comparison between the baseline session and stress level. FD features using medium Gaussian SVM were the highest F1 score for classification between different stress levels (79.92% for classification between L1 and L2, 86.76% for L1 and L3, and 83.40% for L2 and L3). Similar results have been observed in average accuracy with FD features using medium Gaussian SVM is highest compared to WT accuracy results (79.79% for classification between L1 and L2, 84.01% for L1 and L3, and 79.13% for L2 and L3). The results obtained agreed well with the previous works [10], [31].

The results obtained from the fractal dimension classi-

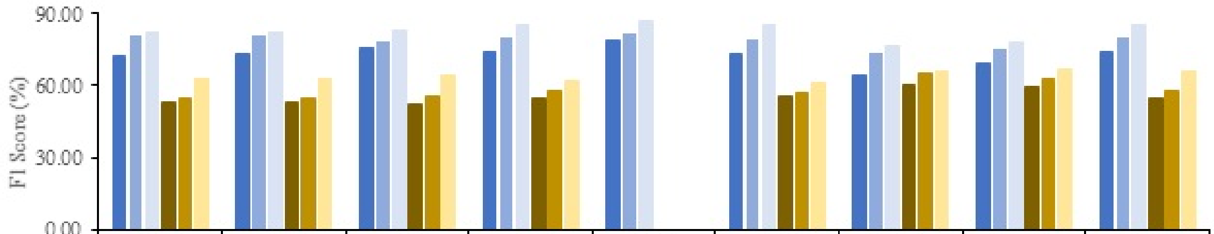

	FT	MT	CT	LD	QD	LR	NBG	NBK	LSVM
FDBS-L1	72.68	72.85	75.47	73.70	78.49	73.59	64.69	68.97	73.87
FDBS-L2	80.95	80.95	78.82	80.12	81.49	79.53	73.75	75.49	80.03
FDBS-L3	82.42	82.38	82.77	85.06	86.89	85.41	76.06	77.89	85.08
WTBS-L1	52.98	52.98	51.93	54.60	0.00	55.53	60.50	59.75	54.58
WTBS-L2	54.57	54.57	55.76	57.65	0.00	57.15	65.14	62.38	57.95
WTBS-L3	62.49	62.49	64.48	61.74	0.00	60.89	65.95	66.40	66.03

(a)

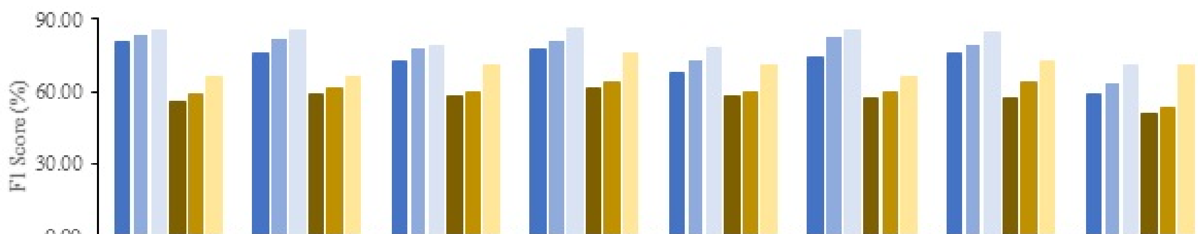

	QSVM	CSVM	FGSVM	MGSVM	CGSVM	FKNN	MKNN	CKNN
FDBS-L1	80.21	75.28	72.59	77.37	68.03	74.19	76.04	58.74
FDBS-L2	83.44	81.43	77.50	81.25	72.74	82.39	79.40	63.15
FDBS-L3	85.44	85.20	78.69	86.17	78.44	85.03	84.72	70.68
WTBS-L1	55.38	59.13	58.30	60.93	58.39	57.03	57.05	50.72
WTBS-L2	59.00	61.11	59.93	63.64	59.39	59.53	63.80	53.26
WTBS-L3	65.98	65.93	70.63	75.55	70.63	65.88	72.35	70.49

(b)

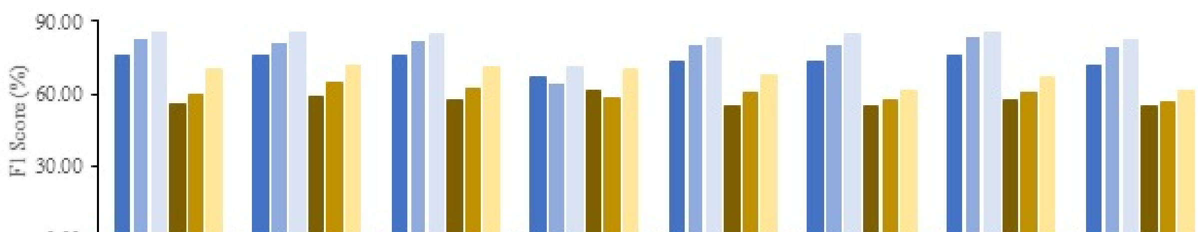

	CsKNN	CbKNN	WKNN	BT	BgT	SD	SKNN	RUSBT
FDBS-L1	75.93	75.96	75.35	67.19	73.28	73.58	75.53	71.77
FDBS-L2	82.81	81.21	81.74	64.33	79.93	79.73	83.34	79.40
FDBS-L3	85.68	85.57	84.79	70.98	82.79	84.25	85.25	82.38
WTBS-L1	55.36	58.70	56.85	61.03	55.19	54.70	57.34	54.88
WTBS-L2	59.95	64.08	62.22	58.11	60.13	57.37	60.73	56.10
WTBS-L3	69.81	71.98	70.97	70.45	67.49	61.49	67.17	61.46

(c)

Figure 4. (a)-(c): Average F1 scores (%) of stress state classification for fractal dimension and wavelet transform features between baseline session and different stress states.

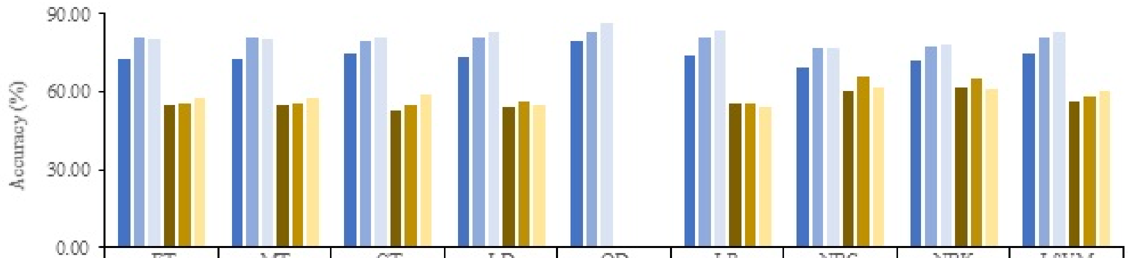

	FT	MT	CT	LD	QD	LR	NBG	NBK	LSVM
FD BS-L1	72.85	72.84	74.55	73.62	79.23	73.74	69.08	71.78	74.37
FD BS-L2	80.83	80.83	79.71	80.99	82.87	80.64	76.76	77.60	80.72
FD BS-L3	80.18	80.15	80.59	83.17	86.27	83.30	76.48	78.01	83.17
WT BS-L1	54.65	54.65	52.67	54.19	0.00	55.29	60.28	61.62	56.03
WT BS-L2	55.20	55.20	54.80	56.42	0.00	55.16	65.61	65.25	58.07
WT BS-L3	57.82	57.82	58.96	54.74	0.00	54.21	61.74	61.06	60.59

(a)

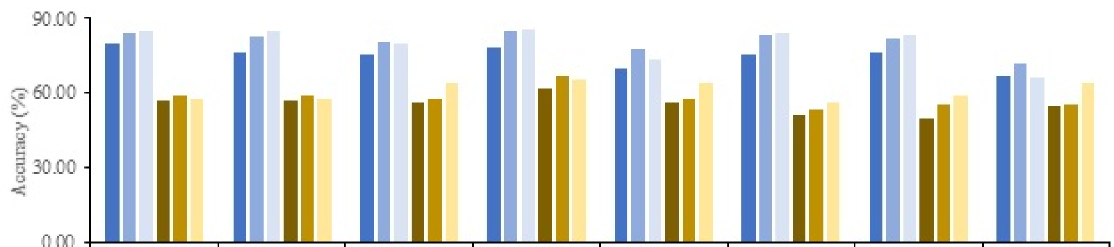

	QSVM	CSVM	FGSVM	MGSVM	CGSVM	FKNN	MKNN	CKNN
FD BS-L1	79.77	75.88	75.60	78.17	69.70	75.17	76.20	67.02
FD BS-L2	84.28	82.74	80.61	84.65	77.84	83.10	81.55	72.14
FD BS-L3	84.69	84.44	79.39	85.79	73.22	84.31	83.23	65.91
WT BS-L1	56.62	56.88	56.02	61.81	56.22	51.01	49.77	54.51
WT BS-L2	59.08	59.18	57.30	66.72	57.30	53.19	55.00	55.36
WT BS-L3	57.19	57.11	63.74	65.54	63.74	56.01	58.84	63.68

(b)

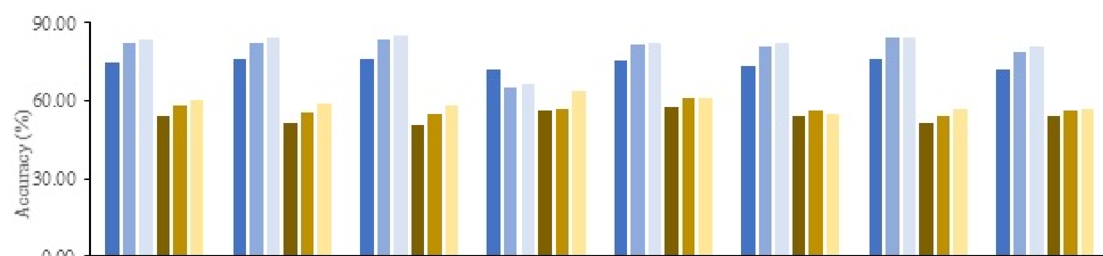

	CsKNN	CbKNN	WKNN	BT	BgT	SD	SKNN	RUSBT
FD BS-L1	74.74	76.02	76.36	72.06	75.11	73.43	76.14	72.27
FD BS-L2	82.08	82.29	83.67	65.37	81.46	80.57	84.15	79.11
FD BS-L3	83.34	84.08	84.68	66.44	82.53	81.97	84.23	80.71
WT BS-L1	54.43	51.06	50.70	56.25	57.37	54.30	51.20	54.19
WT BS-L2	58.18	55.28	55.10	57.10	61.12	56.34	54.18	55.94
WT BS-L3	60.56	58.93	58.15	63.58	60.90	54.63	57.06	56.95

(c)

Figure 5. (a)-(c): Average accuracy (%) of stress state classification for fractal dimension and wavelet transform features between baseline session and different stress states.

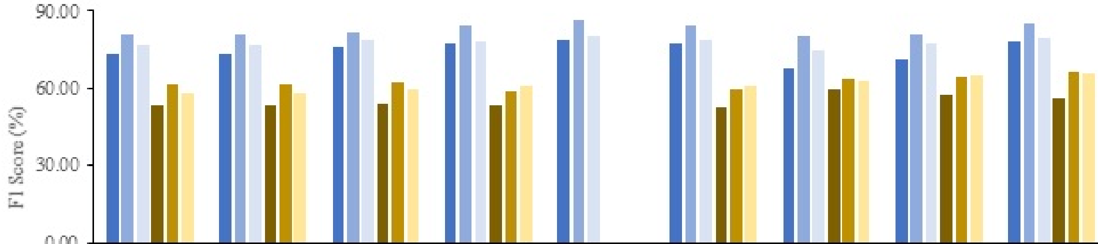

	FT	MT	CT	LD	QD	LR	NBG	NBK	LSVM
FD L1-L2	73.22	73.22	76.19	77.36	78.78	77.31	67.56	71.48	78.29
FD L1-L3	81.11	81.11	81.55	84.32	86.38	83.95	79.93	80.92	84.98
FD L2-L3	76.47	76.47	78.56	78.30	80.33	78.57	74.41	77.18	79.49
WT L1-L2	53.39	53.39	53.70	53.07	0.00	52.47	59.22	57.29	56.13
WT L1-L3	61.18	61.18	62.01	58.51	0.00	59.62	63.66	63.95	66.43
WT L2-L3	58.22	58.22	59.72	60.88	0.00	61.01	62.69	65.21	65.40

(a)

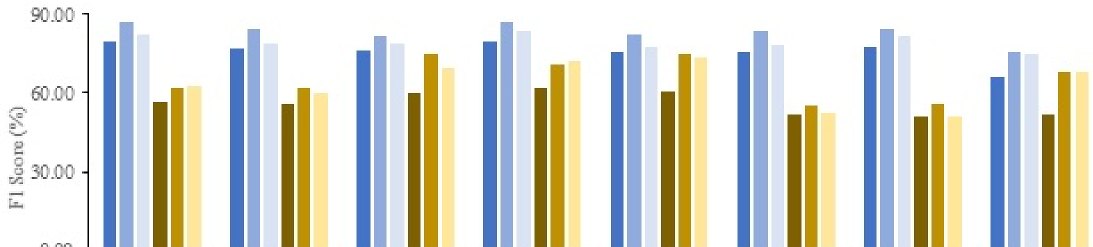

	QSVM	CSVM	FGSVM	MGSVM	CGSVM	FKNN	MKNN	CKNN
FD L1-L2	79.88	76.67	76.36	79.92	75.84	75.78	77.79	65.99
FD L1-L3	86.80	84.57	81.49	86.76	81.99	83.83	84.24	75.38
FD L2-L3	82.00	79.23	78.62	83.40	77.73	78.35	81.49	74.91
WT L1-L2	56.86	55.87	59.68	61.87	60.90	51.70	51.24	51.65
WT L1-L3	61.81	62.09	74.63	70.58	74.63	54.90	55.94	68.21
WT L2-L3	62.45	60.25	69.41	72.46	73.66	52.51	51.27	68.15

(b)

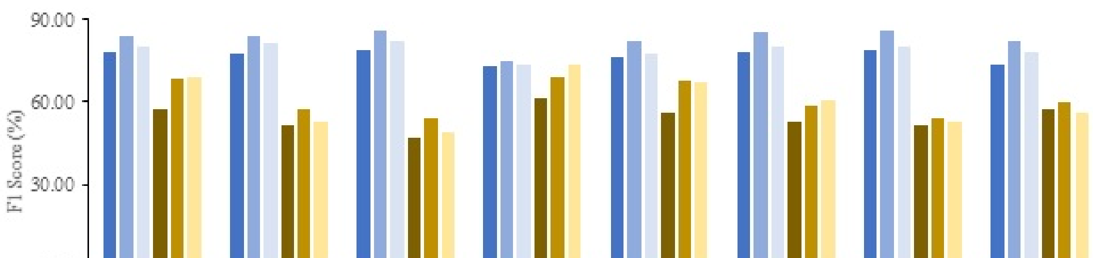

	CsKNN	CbKNN	WKNN	BT	BgT	SD	SKNN	RUSBT
FD L1-L2	77.84	77.60	78.62	72.76	76.06	77.84	78.59	73.53
FD L1-L3	84.14	84.04	85.66	75.14	81.71	85.04	85.91	81.80
FD L2-L3	79.75	81.26	82.22	73.55	77.32	79.90	80.10	77.88
WT L1-L2	57.37	51.64	46.82	61.49	55.78	53.11	51.79	57.66
WT L1-L3	68.52	57.62	54.08	68.76	67.84	58.56	54.03	59.90
WT L2-L3	68.86	52.54	49.14	73.66	66.77	60.90	52.51	55.93

(c)

Figure 6. (a)-(c): Average F1 scores (%) of stress state classification for fractal dimension and wavelet transform feature for different stress state comparisons.

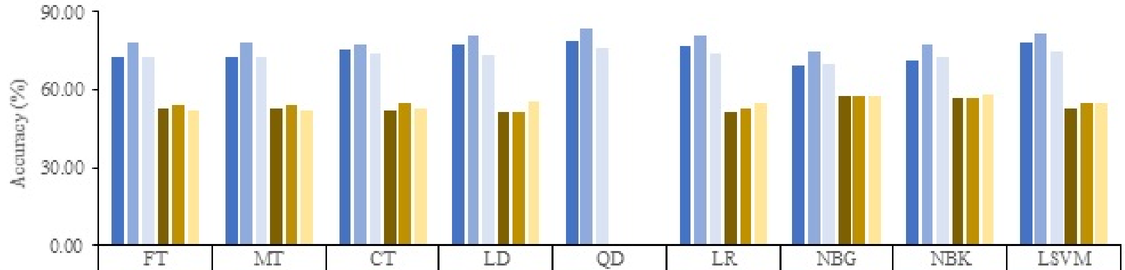

	FT	MT	CT	LD	QD	LR	NBG	NBK	LSVM
FD L1-L2	72.35	72.35	75.09	77.18	78.98	76.99	69.07	71.31	77.99
FD L1-L3	77.88	77.88	77.31	81.05	83.65	80.80	75.00	77.10	81.79
FD L2-L3	72.75	72.75	74.08	73.42	76.09	73.91	69.89	72.54	74.61
WT L1-L2	52.55	52.55	52.13	51.46	0.00	51.09	57.74	56.86	52.69
WT L1-L3	53.95	53.95	54.70	51.04	0.00	52.79	57.46	56.78	54.62
WT L2-L3	52.10	52.10	52.61	55.17	0.00	55.00	57.37	58.47	55.11

(a)

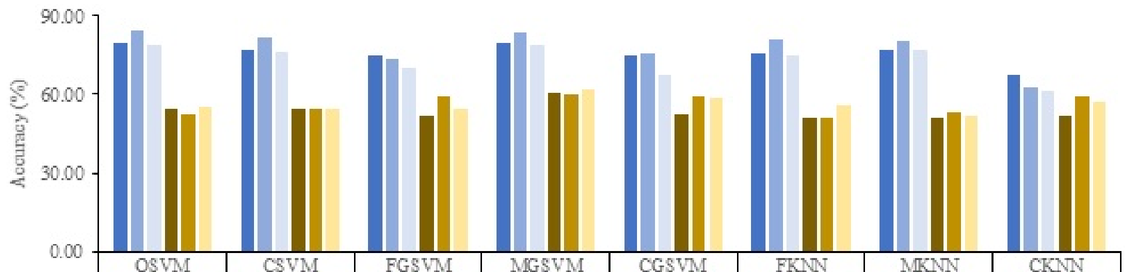

	QSVM	CSVM	FGSVM	MGSVM	CGSVM	FKNN	MKNN	CKNN
FD L1-L2	79.80	76.62	74.76	79.79	74.86	75.24	76.57	67.18
FD L1-L3	84.13	81.77	73.26	84.01	75.52	80.74	79.97	63.01
FD L2-L3	78.62	75.97	69.94	79.13	67.43	74.54	76.67	61.11
WT L1-L2	54.82	54.35	51.98	60.51	52.38	50.93	51.19	51.64
WT L1-L3	52.75	54.45	59.57	59.95	59.57	51.41	53.49	59.08
WT L2-L3	55.39	54.59	54.68	61.72	58.31	55.99	51.53	57.02

(b)

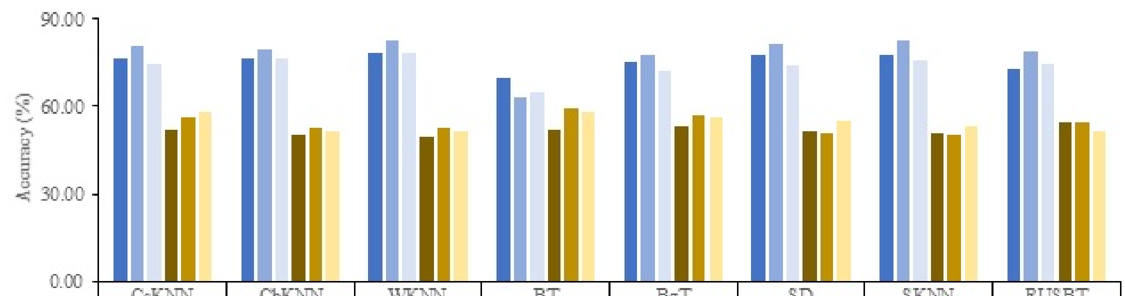

	CsKNN	CbKNN	WKNN	BT	BgT	SD	SKNN	RUSBT
FD L1-L2	76.50	76.39	78.27	69.54	74.90	77.48	77.79	72.59
FD L1-L3	80.50	79.68	82.55	62.74	77.71	81.35	82.68	79.03
FD L2-L3	74.79	76.56	78.43	64.86	72.11	73.97	75.79	74.60
WT L1-L2	52.11	50.13	49.61	52.07	53.34	51.70	50.88	54.79
WT L1-L3	56.49	52.89	52.83	59.57	57.10	51.06	50.25	54.72
WT L2-L3	57.97	51.68	51.76	58.31	56.19	55.17	53.18	51.50

(c)

Figure 7. (a)-(c): Average accuracy (%) of stress state classification for fractal dimension and wavelet transform feature for different stress state comparisons.

fication as a feature using a medium Gaussian SVM ML model derived from the EEG signals suggested that stress state could be classified using this method. Therefore, as future research ideas, we intend to develop a system that automatically determines the stress levels from EEG signals based on the same feature and classification algorithms.

4. Conclusion

This research was devoted to access the capability of the FD and WT method as features for stress state classification using EEG signals. It was found that FD features using ML quadratic SVM have the highest F1 score with 80.% (BS-L1), 83.44% (BS-L2), and 85.44% (BS-L3) in the comparison between baseline session and different stress states. For comparison between different stress states, FD with medium Gaussian SVM as classifier has the highest F1 score with 79.92% (L1-L2), 86.76% (L1-L3), and 83.4% (L2-L3). Future advances in this research would concentrate on the number of subjects and exploring other aspects of the feature extraction methods for the stress states classification.

Acknowledgment

This research is partially supported by the Ministry of Higher Education Malaysia under the Higher Institution Centre of Excellence (HICoE) Scheme and grant for Presenting Academic Paper (UniKL/Cori/conference grant/008-522350), Universiti Kuala Lumpur.

References

[1] L. F. Haas, "Hans Berger (1873-1941), Richard Caton (1842-1926), and electroencephalography," *Journal of Neurology, Neurosurgery & Psychiatry*, vol. 74, no. 1, pp. 9–9, jan 2003. [Online]. Available: https://jnnp.bmj.com/lookup/doi/10.1136/jnnp.74.1.9

[2] A. A. H. Mahmoud, "Effect of Work Stress on EEG Activity in Medical Professionals," *Techniques in Neurosurgery & Neurology*, no. 2, pp. 1–4, 2020.

[3] S. A. Hosseini and M. A. Khalilzadeh, "Emotional Stress Recognition System Using EEG and Psychophysiological Signals: Using New Labelling Process of EEG Signals in Emotional Stress State," in *2010 International Conference on Biomedical Engineering and Computer Science*. IEEE, apr 2010, pp. 1–6.

[4] X. W. Wang, D. Nie, and B. L. Lu, "Emotional state classification from EEG data using machine learning approach," *Neurocomputing*, vol. 129, pp. 94–106, 2014. [Online]. Available: http://dx.doi.org/10.1016/j.neucom.2013.06.046

[5] S. Hwang, H. Jebelli, B. Choi, M. Choi, and S. Lee, "Measuring Workers' Emotional State during Construction Tasks Using Wearable EEG," *Journal of Construction Engineering and Management*, vol. 144, no. 7, p. 04018050, jul 2018. [Online]. Available: http://ascelibrary.org/doi/10.1061/{%}28ASCE{%}29CO.1943-7862.0001506

[6] S. A. Hosseini, M. A. Khalilzadeh, and S. Changiz, "Emotional Stress Recognition System For Affective Computing Based on Bio-Signals," *Journal of Biological Systems*, vol. 18, no. spec01, pp. 101–114, oct 2010. [Online]. Available: https://www.worldscientific.com/doi/abs/10.1142/S0218339010003640

[7] S. Keshmiri, "Conditional entropy: A potential digital marker for stress," *Entropy*, vol. 23, no. 3, p. 286, 2021.

[8] Hasan and Kim, "A Hybrid Feature Pool-Based Emotional Stress State Detection Algorithm Using EEG Signals," *Brain Sciences*, vol. 9, no. 12, p. 376, dec 2019. [Online]. Available: https://www.mdpi.com/2076-3425/9/12/376

[9] S. A. Hosseini, M. A. Khalilzadeh, M. B. Naghibi-Sistani, and V. Niazmand, "Higher Order Spectra Analysis of EEG Signals in Emotional Stress States," in *2010 Second International Conference on Information Technology and Computer Science*. IEEE, jul 2010, pp. 60–63.

[10] X. Hou, Y. Liu, W. L. Lim, Z. Lan, O. Sourina, W. Mueller-Wittig, and L. Wang, "CogniMeter: EEG-Based Brain States Monitoring," in *Transactions on Computational Science XXVIII. Springer Berlin Heidelberg*, ser. Lecture Notes in Computer Science, M. L. Gavrilova, C. K. Tan, and A. Sourin, Eds. Berlin, Heidelberg: Springer Berlin Heidelberg, 2016, vol. 9590, pp. 108–126. [Online]. Available: http://link.springer.com/10.1007/978-3-662-53090-0{_}6

[11] T. K. Calibo, J. A. Blanco, and S. L. Firebaugh, "Cognitive stress recognition," *Conference Record - IEEE Instrumentation and Measurement Technology Conference*, pp. 1471–1475, 2013.

[12] L. Chee-Keong Alfred and W. Chong Chia, "Analysis of Single-Electrode EEG Rhythms Using MATLAB to Elicit Correlation with Cognitive Stress," *International Journal of Computer Theory and Engineering*, vol. 7, no. 2, pp. 149–155, 2015. [Online]. Available: http://www.ijcte.org/index.php?m=content{&}c=index{&}a=show{&}catid=62{&}id=1132

[13] H. Jebelli, S. Hwang, and S. Lee, "EEG-based workers' stress recognition at construction sites," *Automation in Construction*, vol. 93, no. January, pp. 315–324, sep 2018. [Online]. Available: https://linkinghub.elsevier.com/retrieve/pii/S092658051830013X

[14] S. M. U. Saeed, S. M. Anwar, H. Khalid, M. Majid, and U. Bagci, "EEG based classification of long-term stress using psychological labeling," *Sensors (Switzerland)*, vol. 20, no. 7, pp. 1–15, 2020.

[15] NeuroElectrics, "Neuroelectrics User Manual: P1.Enobio," in *Neuroelectrics User Manual*, 2016, vol. 2.3, pp. 1–35.

[16] Neuroelectrics, "Neuroelectrics User Manual: P3.NIC2.0.6," in *Neuroelectrics User Manual*, 2016, vol. 1.4, pp. 1–61.

[17] NeuroElectrics, "Neuroelectrics User Manual: P2.Electrodes," in *Neuroelectrics User Manual*, 2016, vol. 1.3, pp. 1–26.

[18] W.-L. Hu, J. J. Meyer, Z. Wang, T. Reid, D. E. Adams, S. Prabnakar, and A. R. Chaturvedi, "Dynamic Data Driven Approach for Modeling Human Error," *Procedia Computer Science*, vol. 51, pp. 1643–1654, 2015. [Online]. Available: http://www.sciencedirect.com/science/article/pii/S1877050915011060

[19] S. T. Mueller and B. J. Piper, "The Psychology Experiment Building Language (PEBL) and PEBL Test Battery," *Journal of Neuroscience Methods*, vol. 222, pp. 250–259, 2014. [Online]. Available: http://dx.doi.org/10.1016/j.jneumeth.2013.10.024

[20] X. Hou, Y. Liu, O. Sourina, Y. R. E. Tan, L. Wang, and W. Mueller-Wittig, "EEG Based Stress Monitoring," in *2015 IEEE International Conference on Systems, Man, and Cybernetics*, no. November. IEEE, oct 2015, pp. 3110–3115.

[21] S. Gedam and S. Paul, "A Review on Mental Stress Detection using

Wearable Sensors and Machine Learning Techniques," *IEEE Access*, vol. 9, pp. 1–1, 2021.

[22] M. K. Islam, A. Rastegarnia, and Z. Yang, "Methods for artifact detection and removal from scalp EEG: A review," *Neurophysiologie Clinique/Clinical Neurophysiology*, vol. 46, no. 4-5, pp. 287–305, nov 2016. [Online]. Available: https://linkinghub.elsevier.com/retrieve/pii/S098770531630199X

[23] H. Candra, M. Yuwono, Rifai Chai, A. Handojoseno, I. Elamvazuthi, H. T. Nguyen, and S. Su, "Investigation of window size in classification of EEG-emotion signal with wavelet entropy and support vector machine," in *2015 37th Annual International Conference of the IEEE Engineering in Medicine and Biology Society (EMBC)*, vol. 2015-Novem. IEEE, aug 2015, pp. 7250–7253.

[24] X. Hou, F. Trapsilawati, Y. Liu, O. Sourina, C.-H. Chen, W. Mueller-Wittig, and W. T. Ang, "EEG-Based Human Factors Evaluation of Conflict Resolution Aid and Tactile User Interface in Future Air Traffic Control Systems," in *Advances in Human Aspects of Transportation*. Springer, Cham, 2017, vol. 484, no. August 2016, pp. 885–897. [Online]. Available: http://link.springer.com/10.1007/978-3-319-41682-3{_}73

[25] T. Higuchi, "Approach to an irregular time series on the basis of the fractal theory," pp. 277–283, 1988.

[26] H. Adeli, Z. Zhou, and N. Dadmehr, "Analysis of EEG records in an epileptic patient using wavelet transform," *Journal of Neuroscience Methods*, vol. 123, no. 1, pp. 69–87, 2003.

[27] C. Parameswariah and M. Cox, "Frequency characteristics of wavelets," *IEEE Transactions on Power Delivery*, vol. 17, no. 3, pp. 800–804, jul 2002. [Online]. Available: http://ieeexplore.ieee.org/document/1022806/

[28] J. Carp and R. J. Compton, "Alpha power is influenced by performance errors," *Psychophysiology*, vol. 46, no. 2, pp. 336–343, 2009.

[29] A. J. Niemiec and B. J. Lithgow, "Alpha-band characteristics in EEG spectrum indicate reliability of frontal brain asymmetry measures in diagnosis of depression," *Annual International Conference of the IEEE Engineering in Medicine and Biology - Proceedings*, vol. 7 VOLS, pp. 7517–7520, 2005.

[30] W. Klimesch, "EEG alpha and theta oscillations reflect cognitive and memory performance: a review and analysis," *Brain Research Reviews*, vol. 29, no. 2-3, pp. 169–195, apr 1999. [Online]. Available: https://linkinghub.elsevier.com/retrieve/pii/S0165017398000563

[31] S. Fan, J. Zhang, E. Blanco-Davis, Z. Yang, J. Wang, and X. Yan, "Effects of seafarers' emotion on human performance using bridge simulation," *Ocean Engineering*, vol. 170, no. May, pp. 111–119, dec 2018. [Online]. Available: https://linkinghub.elsevier.com/retrieve/pii/S0029801818308102

Fatimah Abdul Hamid Fatimah Abdul Hamid is currently pursuing her part-time Ph.D with Universiti Teknologi PETRONAS and working as a lecturer with the Marine and Electrical Engineering Technology (MEET) Section, Universiti Kuala Lumpur Malaysian Institute of Marine Engineering Technology (UniKL MIMET). She received her B.Eng. (Hons) and master's degree in Electrical, Electronics and System Engineering from Universiti Kebangsaan Malaysia (UKM), Malaysia in 2002 and 2009, respectively. Her research interests include brain science and engineering, machine learning, pattern recognition, feature extraction, and signal processing.

Mohamad Naufal Mohamad Saad Mohamad Naufal Mohamad Saad received the master's degree from the Ecole Nationale Supérieure d'Ingénieurs de Limoges (ENSIL), France, and the Ph.D. degree in telecommunication from the Université de Limoges (UNILIM), France, in 2005. He is currently the Director of International Relations, Universiti Teknologi PETRONAS. His research interests include neuro signal processing, and medical imaging and communication.

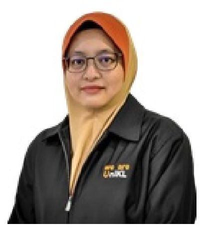

Norshakila Haris Norshakila Haris is currently a Senior Lecturer and a Head of the Quality Assurance (QA) Section. She received the B.Eng. (Hons) degree in Electronics Engineering from Cardiff University of Wales, U.K and the M.Eng. degree in Electrical-Electronics & Telecommunications from Universiti Teknologi Malaysia (UTM), Malaysia in 2006 and 2008, respectively. In 2017, she received her Ph.D. degree in Electrical and Electronics Engineering from The University of Manchester, UK. She has been working with Universiti Kuala Lumpur Malaysian Institute of Marine Engineering Technology (UniKL MIMET) since July 2008. Dr. Norshakila is a Senior Member of IEEE. She was a Secretary of IEEE Student Branch of The University of Manchester, UK from July 2013 until August 2015. Then, she became the first female Chair of the IEEE Student Branch of The University of Manchester from September 2015 until May 2017. Her research interests include three-dimensional multilayer integration and characterisation of CPW MMIC components for future wireless communications. She was among the three recipients who received the GaAs Association Student Fellowship at the 11th European Microwave Integrated Circuits (EuMIC) Conference in London, UK, in 2016. The award was given to recognize and provide financial assistance to international PhD students who show promise and interest in pursuing a graduate degree in microwave electronics.